

Adaptive Routing for Dynamic On-Body Wireless Sensor Networks

Arash Maskooki, Cheong Boon Soh, Erry Gunawan, and Kay Soon Low

Abstract—Energy is scarce in mobile computing devices including wearable and implantable devices in a wireless body area network. In this paper, an adaptive routing protocol is developed and analyzed which minimizes the energy cost per bit of information by using the channel information to choose the best strategy to route data. In this approach, the source node will switch between direct and relayed communication based on the quality of the link and will use the relay only if the channel quality is below a certain threshold. The mathematical model is then validated through simulations which shows that the adaptive routing strategy can improve energy efficiency significantly compared with existing methods.

Index Terms—Adaptive routing, bit error rate (BER) analysis, body area networks (BANs), dynamic channel modeling, indoor communications, radio channel, routing, wireless body sensor network routing, wireless networks, wireless system modeling.

I. INTRODUCTION

PROVIDING ubiquitous connectivity to mobile and wearable computing devices leads to interesting potential applications. For example, a user can enjoy online music streaming through his wireless headphone at home while his blood pressure data are being monitored at a clinic via Internet. However, before such systems enter consumer market, there are a number of challenges that need to be addressed.

Generally, a wireless body area network (WBAN) is a network of heterogeneous wearable and personal computing radio devices with different functionalities and resources. Every network has a network coordinator or hub which is responsible to establish and coordinate the network. Due to the small dimensions and light weight of mobile computing devices, their energy resources are scarce and thus preserving energy is a major design concern. The most energy-efficient strategy to provide connectivity between nodes in a body area network (BAN) and an outside network such as Internet is through a gateway. The network coordinator usually acts as the gateway as it has more computational and power resources. Hence, nodes in a BAN have to connect to the gateway to access outside networks and data [1]–[3].

Manuscript received August 6, 2013; revised January 22, 2014; accepted March 17, 2014. Date of publication March 24, 2014; date of current version March 2, 2015.

The authors are with the School of Electrical and Electronics Engineering, Nanyang Technological University, Singapore 639798 (e-mail: aras0004@e.ntu.edu.sg; ecbsoh@ntu.edu.sg; egunawan@ntu.edu.sg; ekslow@ntu.edu.sg).

Color versions of one or more of the figures in this paper are available online at <http://ieeexplore.ieee.org>.

Digital Object Identifier 10.1109/JBHI.2014.2313343

Before the introduction of IEEE 802.15.6 standard for a BAN, most of the efforts in WBAN analysis were focused on improving the best candidate for low-power short-range communication standard, IEEE 802.15.4. In [4], the performance of IEEE 802.15.4 in beacon mode is analyzed for single-hop BANs. The use of IEEE 802.15.4 standard in an ECG-monitoring BAN is studied in terms of the sampling rate, transmitting cycles, and number of network devices in [5]. The effect of the payload size on the latency and packet delivery rate is analyzed. In [6], an energy-efficient protocol for a BAN is proposed and compared with IEEE 802.15.4 MAC protocol in contention-free TDMA access mode. The proposed protocol can improve energy efficiency by 10%. In [7], using extra nodes and cooperation between nodes to relay information to the base is compared with the single-hop scheme. Simulation results show that the relay network can greatly improve the lifetime of the network. Network lifetime is defined as the time interval between the time network starts working to the time in which the first node dies in the network. It has been shown that in the single-hop scheme the nodes with highest distance from the sink will be drained out of energy faster, while in the multihop case the relay nodes closer to the sink have much higher energy consumption due to the traffic they carry.

IEEE 802.15.6 standard has recently been published for wireless communication in short vicinity or inside the human body [8]. The main objective of this standard is to provide connectivity between low-power wearable and implanted devices while supporting high data rates (up to 10 Mbps) as well as quality of service. Two types of the network topologies are specified in the standard. The first type is the star topology where all nodes connect directly to the hub. The second topology is the two-hop extended star topology where nodes and hub can exchange information through a relay node. To connect through the relay, the nodes and the hub encapsulate their data and management frames in the payload of another frame with the same type and transmit to the relay and the relay retransmits the encapsulated frame to the destination. Transmissions to and from the relay are performed using the direct communication rules specified in the standard. Throughput and delay of systems working based on IEEE 802.15.6 are analyzed and compared with simulation results in [9]–[14]. In [15], a MAC protocol is proposed for ultralow data rate energy-harvesting devices which allows for longer sleeping time and hence lower power consumption during beacon mode of IEEE 802.15.6 standard. The performance of the IEEE 802.15.6 WBAN single-hop MAC protocol is evaluated in terms of throughput, power consumption, and energy efficiency under unsaturated conditions in [16]. In [17], the performance of the standard is analyzed over the fading channel.

As an example of a futuristic application, consider a patient who has a blood pressure sensor on his wrist which sends regular data to a central device on his waist. In addition, he has a blood flow monitor on his foot which also sends regular data to the central device. Assume both devices are capable of relaying data from other nodes. The standard suggests the use of either single-hop or two-hop schemes to route data to the central device. However, the human body is a dynamic environment and the characteristics of the channel change by time [18]. As a result, using a fixed scheme is not the optimum strategy in dynamic and time-varying environments such as a human body. When the quality of the channel is higher than a threshold, using a relay channel unnecessarily increases the energy cost, i.e., the relay channel is needed only in severe fading conditions. In our scenario, the device on the wrist occasionally experiences high quality link with the central device and hence using a direct path is more energy efficient than any relay path. On the other hand, during the hand movements, the link quality may suffer severe fading due to the blocking by the human body and hence using the relay path would be inevitable. In this paper, an adaptive cross layer protocol is introduced which exploits the channel information at the transmitter side to decide on the best routing strategy. In this approach, a transmitter obtains information on the channel through a feedback and decides whether to use an alternate relay channel to create redundancy. Mathematical analysis and simulations based on the IEEE 802.15.6 MAC function and channel measurements around a dynamic human body confirm the advantages of the adaptive routing strategy in conserving on-body sensors energy.

This paper has three major contributions.

- 1) An analytical model for the transmission energy cost per bit of information is developed based on the Markov chain of the process and the model is validated through simulations.
- 2) A power-efficient adaptive routing protocol is proposed and the performance of the protocol in terms of energy efficiency and outage is evaluated and compared with the standard in system level through mathematical analysis and simulations.
- 3) A statistical model for the received energy in a dynamic BAN is provided through real-time, time-domain measurements.

This paper is organized as follows: this section introduces strategies and standards to provide connectivity to nodes in a BAN, and the pros and cons of using each method. Adaptive routing protocol will be described and analyzed mathematically in Section II. In Section III, a statistical model for the received power in dynamic on-body channels will be developed based on real-time measurements. The mathematical energy model will be validated in system level and the performance of the adaptive scheme will be compared with the standard in Section IV. Finally, Section V concludes this paper.

II. ADAPTIVE ROUTING

General format of a physical-layer protocol data unit (PPDU) is shown in Fig. 1. The size of each section is shown above

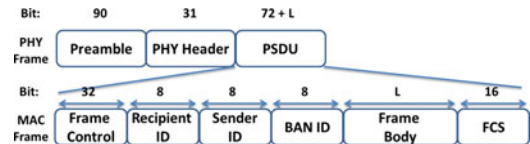


Fig. 1. General format of a PPDU and PSDU.

the section in bits. The PHY layer adds a preamble and its own header to the physical-layer data unit (PSDU) which is delivered by a MAC layer. The PHY header contains transmission information including the data rate and the length of the data. PSDU is the MAC layer frame and consist of six sections as shown in Fig. 1. Frame control section contains information about the frame including the frame type and sequence number of the frame. Recipient ID, sender ID, and BAN ID fields contain the abbreviated address of the intended recipient of the frame, sender of the frame, and the network respectively. The MAC frame body contains the payload information and is not present in control frame types. The length of the MAC frame body varies between 1 and L_{max} . The frame check sequence contains the binary coefficients of a cyclic redundancy check polynomial of degree 15. Details of the frame format and fields are available in [8].

In this paper, to accommodate for the best transmission scheme selection, the CSMA/CA mode of multiple access protocol in IEEE 802.15.6 [8] is extended as described in the rest of this section.

Here, we assume that the request to send/clear to send (RTS/CTS) scheme specified in [19] is used to reserve the medium for data frame exchange. It has been shown that the RTS/CTS scheme can greatly reduce collision time when the payload size is large [20]. To exchange a data frame with the hub (H) directly, the source node (S) initializes a back-off counter with a random integer number between 1 and w_k after sensing that the medium is idle for a contention interframe spacing (CIFS) time interval. k in w_k indicates the number of previous unsuccessful retransmissions of the same frame. w_k is an integer starting from w_0 , doubling even k and saturates at w_m , where $\{w_0, w_m\}$ depend on the user priority of the source node. The counter freezes if the medium is sensed busy during the count down until the end of the current on-going session. If the medium is idle and the back-off counter reaches zero, the source node transmits a request to send (RTS) frame and waits for a clear to send (CTS) frame. If an RTS frame arrives after a short-interframe spacing (SIFS), the source node will transmit its data with another SIFS delay and waits for acknowledgment (ACK) frame from the hub. SIFS is shorter than CIFS to ensure completion of the current session before other nodes start their transmission. As mentioned earlier, if an expected frame (CTS or ACK) is not received from the hub after an SIFS + TO, where TO is the time out interval, the frame is considered lost. In this case, w_k is doubled if the number of retries is even and remains unchanged if it is odd or maximum window size, w_m , is reached.

In adaptive routing, the source node obtains the instantaneous channel information through preamble of the RTS frame

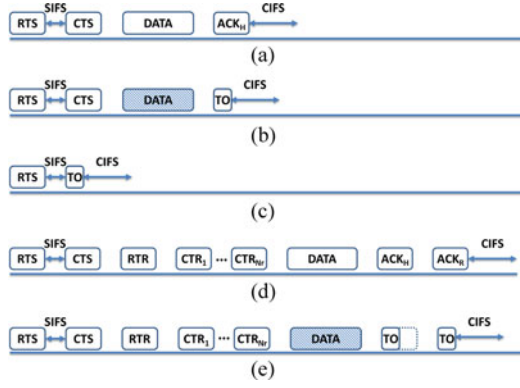


Fig. 2. Sessions corresponding to the data frame transmission in adaptive routing. (a) Successful data frame transmission (Direct). (b) Failed data frame transmission (Direct). (c) Collision. (d) Successful data frame transmission (Relayed). (e) Failed data frame transmission (Relayed).

received from the hub. If the instantaneous channel gain (α) is higher than a threshold (α_0), S uses a direct communication scheme as described previously. On the other hand, if the reception is below the threshold, S transmits a request to relay (RTR) frame after an SIFS. RTR is an RTS frame with the relay field in the frame control header set to 1 and the recipient address set to multicast address of the group of relay nodes. Relays will respond by a clear to relay (CTR) after an SIFS and according to their predefined order number. After receiving the CTR frames from all of the relays, S transmits its encapsulated data frame with recipient ID set as the ID of the relay node with the best link quality and relay field of the header set to 1 to indicate that the final destination is H . If the hub and the chosen relay node (R_i) receive the frame correctly, they will transmit ACK after an SIFS and $2\text{SIFS} + T_{\text{ACK}}$ respectively, where, T_{ACK} is the duration of the ACK frame. If the relay receives the ACK from the hub, it discards the frame. Otherwise, it transmits the data frame to H in a contended session. If S receives an ACK from either H or R_i or both it proceeds to the next frame, otherwise, the frame is considered lost and it tries to retransmit the frame until retry number of the frame reaches maximum or the frame is sent successfully. Fig. 2 shows successful and unsuccessful data transmission sessions with and without a relay.

The bit error rate (BER) requirement of the system depends on the application. For example, in audio streaming applications, a BER level up to 10^{-3} is tolerated while in video streaming applications the BER level must be maintained at 10^{-6} . Here, we assume that the transmitter is able to adjust its transmission power to maintain a certain BER level, e_b , required by higher layers. The preamble of the frames is transmitted with a constant predefined power P_{TX0} .

Assuming that the transmitted bits are independent, the packet error probability of a data frame is

$$p_d = 1 - (1 - e_b)^{N_b}, \quad (1)$$

where N_b is the number of bits in the frame.

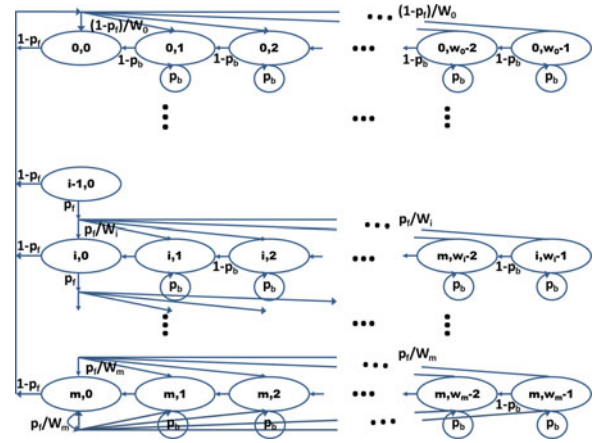


Fig. 3. Markov model of the protocol.

A. Markov Model

A Markov model for IEEE 802.11 DCF function is proposed and analyzed in [20]. This model is extended in [21] to include the freezing of the back-off counter due to an on-going communication. The Markov model in these works is analyzed under a perfect channel. In this paper, we modify the Markov model in [21] to incorporate the differences in the IEEE 802.15.6 MAC layer and variations in the channel quality. This Markov model will be analyzed in the fading channel model discussed in Section III. Similar to the 802.11 DCF function, the maximum back-off number is doubled with failure in the packet delivery. However, this increase occurs even in every failed attempt in IEEE 802.15.6. Applications are prioritized in 802.15.6 to support different delay and throughput requirements. As the main goal in this paper is to analyze the adaptive protocol discussed earlier, we assume that all nodes have the same priority level. In addition, we assume that the error probability of short control frames are negligible compared to the lengthy data frames. To achieve the lower packet error rate for control frames, an error correction code may be implemented in the payload section of the frames.

The Markov model of the protocol is shown in Fig. 3. Rows in Fig. 3 show the back-off stages where w_i indicates the maximum back off number in i th stage and m is maximum number of back off stages. m is always an odd number as if m was even, $w_{m+1} = w_m$ and thus $m + 1$ would be the maximum stage. p_b and p_f are the probabilities of a busy medium and a failed transmission, respectively. A transmission is considered failed if the source node could not verify the reception of the packet by the immediate destination. Similarly, as assumed in [20], p_b is not a function of back off stage of the node and thus is constant. p_b is also the probability of collision. It is worthwhile to note that p_d is the probability that the packet is received with an error due to the undesirable channel condition, while p_b is the probability of the packet loss due to a collision which may occur even in a perfect channel condition. p_f is related to both p_b and p_d , and depends on the routing scheme used by the source node. p_f at

the source node for different schemes is as follows:

$$p_f = \begin{cases} p_b + (1 - p_b)p_d, & \text{Single hop} \\ p_b + (1 - p_b)p_d, & \text{Two-hop} \\ p_b + (1 - p_b)p_d(p_R p_a + (1 - p_R)) & \text{Adaptive,} \end{cases} \quad (2)$$

$$\Rightarrow \frac{b_{0,0}}{2(1 - p_b)} \left[\underbrace{\sum_{i=0}^{m-1} (p_f^i w_i + p_f^i)}_{S_1} + \frac{p_f^m}{1 - p_f} (w_m + 1) \right] = 1 \quad (7)$$

where p_a is the average packet error probability of the direct transmission link between the source node and the hub during a relayed transmission and approximates the instantaneous packet error probability. In a two-hop scheme, p_f is defined on every single hop and hence is equal to the single-hop scheme. p_R is the probability that the source node decides to use relay for data transmission

$$p_R = \int_0^{\alpha_0} f_{SH}(\alpha) d\alpha. \quad (3)$$

in which $f_{SH}(\alpha)$ is the distribution of the gain of the channel between S and H and is obtained in Section III. α_0 is the threshold at which the source node decides to use the relay path instead of a direct link. p_f for the relay node is the same as single hop as the relay will always use the single-hop scheme to communicate with both the source node and the hub.

In the single-hop communication, a transmission session fails either because of a collision or an error in the data packet. In two-hop communication, the packet transmission fails due to channel imperfections or collisions in either of the two hops. In adaptive routing, the probability of a failed transmission depends on whether the source node decides to send the packet directly or through a relay. As both relay and the hub listen for the packet when relay is used, packet delivery fails only if both relay and the hub receive the packet with an error. In a perfect channel, for all schemes, p_d is zero and thus $p_f = p_b$.

The following equations hold for the steady state of the Markov model in Fig. 3 where all the nodes have a packet to transmit immediately after their packet is successfully transmitted or dropped when maximum number of retries is reached. Assume that $b_{i,k}$ is the steady-state probability of the node being in (i, k) th state. Then [21],

$$b_{i,k} = \frac{w_i - k}{w_i(1 - p_b)} b_{i,0} \quad 0 \leq i \leq m. \quad (4)$$

Normalization condition requires that

$$\sum_{i=0}^m \sum_{k=0}^{w_i-1} b_{i,k} = 1. \quad (5)$$

Therefore,

$$\sum_{i=0}^m \frac{b_{i,0}}{1 - p_b} \underbrace{\sum_{k=0}^{w_i-1} \frac{w_i - k}{w_i}}_{\frac{w_i+1}{2}} = 1 \quad (6)$$

from Markov steady-state equations [21] and (6) we obtain

$$\sum_{i=0}^{m-1} \left(\frac{w_i + 1}{2} \frac{b_{i,0}}{1 - p_b} \right) + \frac{w_m + 1}{2} \frac{p_f^m}{1 - p_f} \frac{b_{0,0}}{1 - p_b} = 1;$$

using the fact that $w_{2i} = 2^i w_0$ and $w_{2i+1} = 2^i w_0$ for $i = 0, \dots, (m-1)/2$; we can rewrite S_1 in the above equation as

$$S_1 = \sum_{i=0}^{(m-1)/2} \left(p_f^{2i+1} w_{2i+1} + p_f^{2i+1} + p_f^{2i} w_{2i} + p_f^{2i} \right) \quad (8)$$

$$= (1 + p_f) \left(w_0 \frac{1 - (\sqrt{2} p_f)^{m+1}}{1 - 2p_f^2} + \frac{1 - p_f^{m+1}}{1 - p_f^2} \right). \quad (9)$$

Using (8) in (7) results in

$$b_{0,0} = \frac{2(1 - p_b)}{(1 + p_f) \left(w_0 \frac{1 - (\sqrt{2} p_f)^{m+1}}{1 - 2p_f^2} + \frac{1 - p_f^{m+1}}{1 - p_f^2} \right) + \frac{p_f^m}{1 - p_f} \left(2^{\frac{m-1}{2}} w_0 + 1 \right)}. \quad (10)$$

A node will transmit if its counter reaches zero, and hence, the probability of transmission τ is

$$\tau = \sum_{i=0}^m b_{i,0} = \frac{2(1 - p_b)}{(1 - p_f^2) w_0 \frac{1 - (\sqrt{2} p_f)^{m+1}}{1 - 2p_f^2} + 1 - p_f^{m+1} + p_f^m (1 + p_f) \left(2^{\frac{m-1}{2}} w_0 + 1 \right)}. \quad (11)$$

B. Energy Consumption Analytical Model

To operate in the CSMA/CA mode of IEEE 802.15.6, all nodes must sense the medium at all times and postpone their transmission based on the expected transmission duration of the current frame exchange based on the information provided in the control section of the frames. Thus, the nodes are either listening to the medium or transmitting a frame. Electronics power consumptions is assumed to be included in the corresponding transmit and receive power values. To perform the back off procedure, every node spends some time in the back off states. Assuming a limited number of unsuccessful retries, r_m , after which the packet is dropped, the average number of slots spent in the back off procedure before a packet is successfully transmitted or dropped is given by the following equations. In case $r_m > m$,

$$\bar{n} = \sum_{r=0}^{m-1} p_f^r (1 - p_f) \sum_{k=0}^r \sum_{i=0}^{w_k-1} \frac{1}{w_k} i + \sum_{r=m}^{r_m-1} p_f^r (1 - p_f) \sum_{k=0}^m \sum_{i=0}^{w_k-1} \frac{1}{w_k} i + p_f^{r_m} \sum_{k=0}^m \sum_{i=0}^{w_k-1} \frac{1}{w_k} i. \quad (12)$$

else if $r_m \leq m$,

$$\bar{n} = \sum_{r=0}^{r_m-1} p_f^r (1-p_f) \sum_{k=0}^r \frac{w_k-1}{2} + p_f^{r_m} \sum_{k=0}^{r_m} \frac{w_k-1}{2}. \quad (13)$$

The average energy consumed by the nodes while performing the back off procedure is

$$\bar{E}_{bo} = \bar{n} \beta P_{RX}, \quad (14)$$

where β and P_{RX} are the slot time and the power consumed by the node to receive and overhear the frames on the air, respectively.

The average number of times the channel is sensed busy at each back off state is

$$\bar{s} = \sum_{i=0}^{\infty} (1-p_b) p_b^i = \frac{p_b}{1-p_b}. \quad (15)$$

Hence, the total number of times the channel is sensed busy by a node during the back off procedure is

$$\bar{n}_b = \bar{n} \bar{s}. \quad (16)$$

1) *Source Node*: The energy consumed by the source node while overhearing the on-going transmission depends on whether a collision occurs or not. In case no collision occurs, the packet transmission might be successful or with errors. The average energy of consumption due to overhearing on-going packets during back off procedure is calculated as

$$\bar{E}_o^S = \bar{n}_b \left[\frac{p_b}{p_{tx}} \bar{E}_{oc} + \left(1 - \frac{p_b}{p_{tx}}\right) \left((1-p_d) \bar{E}_{os} + p_d \bar{E}_{of} \right) \right], \quad (17)$$

where p_{tx} is the probability that at least one node is transmitting given by

$$p_{tx} = 1 - (1-\tau)^{N_n}, \quad (18)$$

where N_n is the total number of nodes in the network. \bar{E}_{oc} , \bar{E}_{os} , and \bar{E}_{of} are the energy consumed by a node to overhear a collision, successful data transmission, and failed data transmission by other nodes, respectively, and are calculated as follows:

$$\begin{aligned} \bar{E}_{oc} &= (T_{RTS} + TO + SIFS + CIFS) P_{RX}, \\ \bar{E}_{os} &= (T_{RTS} + T_{CTS} + T_D + T_{ACK} + 3SIFS + CIFS) P_{RX}, \\ \bar{E}_{of} &= (T_{RTS} + T_{CTS} + T_D + TO + 3SIFS + CIFS) P_{RX}, \end{aligned} \quad (19)$$

where, T_{RTS} , T_{CTS} , T_{ACK} , and T_D are duration of RTS, CTS, ACK, and data frames, respectively, including PHY and MAC layer headers.

The average number of retries before a packet is successfully transmitted or dropped is

$$\begin{aligned} \bar{r} &= \sum_{r=0}^{r_m-1} r p_f^r (1-p_f) + p_f^{r_m} r_m \\ &= p_f \frac{1 - r_m p_f^{r_m-1} + (r_m-1) p_f^{r_m}}{1-p_f} + p_f^{r_m} r_m. \end{aligned} \quad (20)$$

The average energy consumed during retransmission is

$$\bar{E}_r^S = \begin{cases} \bar{r} \left[\frac{p_b}{p_f} \bar{E}_{TXc}^S + \left(1 - \frac{p_b}{p_f}\right) \bar{E}_{TXf}^S \right] & \text{Single hop} \\ \bar{r} \left[\frac{p_b}{p_f} \bar{E}_{TXc}^S + \left(1 - \frac{p_b}{p_f}\right) \bar{E}_{TXfR}^S \right] & \text{Two-hop} \\ \bar{r} \left[\frac{p_b}{p_f} \bar{E}_{TXc}^S + \left(1 - \frac{p_b}{p_f}\right) \left(p_R \bar{E}_{TXfR}^S + (1-p_R) \bar{E}_{TXf}^S \right) \right] & \text{Adaptive.} \end{cases} \quad (21)$$

\bar{E}_{TXc}^S , \bar{E}_{TXf}^S , and \bar{E}_{TXfR}^S are the transmission energy consumed during a collision, failed direct data exchange, and failed relayed data frame exchange, respectively, and are obtained as follows:

$$\begin{aligned} \bar{E}_{TXc}^S &= T_{RTS} \bar{P}_{TX}^{SH} + (TO + SIFS + CIFS) P_{RX}, \\ \bar{E}_{TXf}^S &= (T_{RTS} + T_D) \bar{P}_{TX}^{SH} + (T_{CTS} + TO + 3SIFS + CIFS) P_{RX}, \\ \bar{E}_{TXfR}^S &= \end{aligned}$$

$$\begin{cases} (T_{RTS} + T_D) \bar{P}_{TX}^{SR} + (TO + SIFS + CIFS) P_{RX}, & \text{Two-hop} \\ (T_{RTS} + T_{RTR}) \bar{P}_{TX}^{SH} + T_D \bar{P}_{TX}^{SR} + & \text{Adaptive} \\ (T_{CTS} + T_{ACK} + v T_{CTR} + (5+v) SIFS + CIFS) P_{RX}, & \end{cases} \quad (22)$$

where T_{RTR} is the duration of RTR frame. \bar{P}_{TX}^{SH} and \bar{P}_{TX}^{SR} are the average transmission power used by S to maintain the desired BER at H and R , respectively, while transmitting directly

$$\bar{P}_{TX}^{SH} = \int_{\alpha_0}^1 f_{SH}(\alpha) P_{TX}^{SH}(\alpha) d\alpha \quad (23)$$

where P_{TX}^{SH} is the instantaneous power used by S to maintain desired BER at H and,

$$\bar{P}_{TX}^{SR} = \begin{cases} \int_0^1 f_{SR_i}(\alpha) P_{TX}^{SR_i}(\alpha) d\alpha, & \text{Two-hop using } R_i \\ \sum_{i=1}^v p_{R_i} \int_0^1 f_{SR_i}(\alpha) P_{TX}^{SR_i}(\alpha) d\alpha & \text{Adaptive} \end{cases} \quad (24)$$

where p_{R_i} in the adaptive scheme is the probability that R_i is chosen by S over the other relays and is defined as follows:

$$p_{R_i} = p(\alpha_{SR_i} > \alpha_{SR_j}), \quad 1 \leq j \leq N_r, j \neq i, \quad (25)$$

where α_{SR_i} and α_{SR_j} are the gain of the channel between S and i th and j th relay, respectively. N_r is the number of the relays. The probability that a packet is dropped is

$$p_w = 1 - \sum_{r=1}^{r_m} (1-p_f) p_f^{r-1} = p_f^{r_m} \quad (26)$$

and hence, a packet is successfully transmitted with probability

$$p_s = 1 - p_w = 1 - p_f^{r_m}. \quad (27)$$

The average energy consumed to transmit a packet successfully is

$$\bar{E}_s^S = \begin{cases} p_s \bar{E}_{TXs}^S & \text{Single hop} \\ p_s \bar{E}_{TXsR}^S & \text{Two-hop} \\ p_s (p_R \bar{E}_{TXsR}^S + (1 - p_R) \bar{E}_{TXs}^S) & \text{Adaptive} \end{cases} \quad (28)$$

where \bar{E}_{TXs}^S and \bar{E}_{TXsR}^S are the energy consumed during a successful transmission to the hub and relay, respectively, and are obtained through the following equations:

$$\begin{aligned} \bar{E}_{TXs}^S &= (T_{RTS} + T_D) \bar{P}_{TX}^{SH} + (T_{CTS} + T_{ACK} + 3SIFS \\ &+ CIFS) P_{RX}, \\ \bar{E}_{TXsR}^S &= \begin{cases} (T_{RTS} + T_D) \bar{P}_{TX}^{SR} + (T_{CTS} + T_{ACK} + 3SIFS \\ + CIFS) P_{RX} & \text{Two-hop} \\ (T_{RTS} + T_{RTR}) \bar{P}_{TX}^{SH} + T_D \bar{P}_{TX}^{SR} + (T_{CTS} + vT_{CTR} + \\ 2T_{ACK} + (5 + v)SIFS + CIFS) P_{RX} & \text{Adaptive.} \end{cases} \end{aligned} \quad (29)$$

The average total energy consumed by the source node per data bit is

$$\bar{E}_b^S = \frac{\bar{E}_{bo} + \bar{E}_o^S + \bar{E}_r^S + \bar{E}_s^S}{L} \quad (30)$$

where L is the payload size.

2) *Relay Node*: Relay node sends the packet received from S in the single-hop scheme. The average energy consumed by the relay R_i to receive a packet from S is

$$\bar{E}_{RX}^{R_i} = (1 - p_d) \bar{E}_{RXs}^{R_i} + p_d \bar{E}_{RXf}^{R_i} \quad (31)$$

where $\bar{E}_{RXs}^{R_i}$ and $\bar{E}_{RXf}^{R_i}$ are energy consumption for receiving a successful or failed data packet and are obtained as

$$\begin{aligned} \bar{E}_{RXs}^{R_i} &= \begin{cases} (T_{CTS} + T_{ACK}) \bar{P}_{TX}^{R_iS} + (T_{RTS} + T_D \\ + T_{ACK} + 4SIFS + CIFS) P_{RX} & \text{Two-hop} \\ (T_{CTR} + T_{ACK}) \bar{P}_{TX}^{R_iS} + (T_{RTR} + (v - 1)T_{CTR} + T_D \\ + T_{ACK} + (4 + v)SIFS + CIFS) P_{RX} & \text{Adaptive} \end{cases} \quad (32) \\ \bar{E}_{RXf}^{R_i} &= \begin{cases} T_{CTS} \bar{P}_{TX}^{R_iS} + (T_{RTS} + T_D + TO \\ + 3SIFS + CIFS) P_{RX} & \text{Two-hop} \\ T_{CTR} \bar{P}_{TX}^{R_iS} + (T_{RTR} + (v - 1)T_{CTR} + T_D + TO \\ + (v + 3)SIFS + CIFS) P_{RX} & \text{Adaptive,} \end{cases} \end{aligned} \quad (33)$$

where $\bar{P}_{TX}^{R_iS}$ is the average transmission power of R_i used to transmit to S .

As required by the IEEE 802.15.6 standard, in the CSMA/CA mode, nodes must listen to the medium to sense the busy medium and perform the back off procedure in case they need to transmit a frame. The average energy consumed by R_i to overhear an ongoing communications is

$$\bar{E}_o^{R_i} = \bar{n}_b \left[\frac{p_b}{p_{tx}} \bar{E}_{oc} + \left(1 - \frac{p_b}{p_{tx}}\right) ((1 - p_d) \bar{E}_{os} + p_d \bar{E}_{of}) \right]. \quad (34)$$

The average energy consumed during retransmissions is

$$\bar{E}_r^{R_i} = \bar{r} \left[\frac{p_b}{p_f} \bar{E}_{TXc}^{R_i} + \left(1 - \frac{p_b}{p_f}\right) \bar{E}_{TXf}^{R_i} \right]. \quad (35)$$

\bar{E}_{TXc}^S and \bar{E}_{TXf}^S are the average transmission energy consumed during a collision and failed data frame exchange, respectively, and are obtained as follows:

$$\begin{aligned} \bar{E}_{TXc}^{R_i} &= T_{RTS} \bar{P}_{TX}^{R_iH} + (TO + SIFS + CIFS) P_{RX}, \\ \bar{E}_{TXf}^{R_i} &= (T_{RTS} + T_D) \bar{P}_{TX}^{R_iH} + (T_{CTS} + TO + 3SIFS \\ &+ CIFS) P_{RX}, \end{aligned} \quad (36)$$

where $\bar{P}_{TX}^{R_iH}$ is the average transmission power of R_i used to transmit to H .

The average energy consumed to transmit a packet successfully is

$$\bar{E}_s^{R_i} = p_s \bar{E}_{TXs}^{R_i} \quad (37)$$

where $\bar{E}_{TXs}^{R_i}$ is the energy consumed during a successful transmission and is obtained through the following equation:

$$\begin{aligned} \bar{E}_{TXs}^{R_i} &= (T_{RTS} + T_D) \bar{P}_{TX}^{R_iH} + (T_{CTS} + T_{ACK} + 3SIFS \\ &+ CIFS) P_{RX}. \end{aligned} \quad (38)$$

The average total energy consumed by the relay node per data bit is

$$\bar{E}_b^{R_i} = \frac{\bar{E}_{RX}^{R_i} + (1 - p_d)(\bar{E}_{bo} + \bar{E}_o^{R_i} + \bar{E}_r^{R_i} + \bar{E}_s^{R_i})}{L}. \quad (39)$$

As a result, the average total energy consumed on a payload bit is

$$\bar{E}_b^T = \begin{cases} \bar{E}_b^S, & \text{Single hop} \\ \bar{E}_b^S + \bar{E}_b^{R_i}, & \text{Two-hop using } R_i \\ \bar{E}_b^S + p_R \sum_{i=1}^v p_{R_i} \bar{E}_b^{R_i} & \text{Adaptive.} \end{cases} \quad (40)$$

To obtain a measure of the reliability of the network, we define the outage as the probability that a data packet transmission is unsuccessful and is dropped by the transmitter after maximum number of retries is reached. The outage probabilities of single-hop, two-hop, and adaptive are as follows:

$$p_o = \begin{cases} p_f^m, & \text{Single hop} \\ p_f^m + (1 - p_f^m) p_f^m, & \text{Two-hop} \\ p_{f_s}^m + (1 - p_{f_s}^m) p_R p_a p_{f_r}^m & \text{Adaptive,} \end{cases} \quad (41)$$

where p_{f_s} and p_{f_r} are the probability of a failed transmission by the source node using adaptive routing and the relay node using the single-hop scheme, respectively, as given in (2). In a two-hop communication, outage as defined previously occurs either when the source node drops the data after reaching maximum retries or when the packet is successfully transmitted to the relay but is later dropped by the relay. In adaptive routing, outage occurs when neither the relay nor the hub receive the data or when only the relay receives the packet successfully but later drops the packet due to the maximum retry limit.

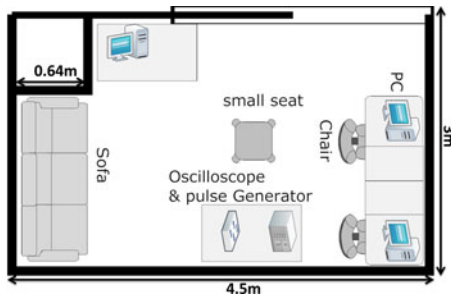


Fig. 4. Experiment room plan.

III. CHANNEL MODEL

Statistics of the channel quality is obtained through time-domain measurements using an Agilent Infiniium DSO80804B real-time oscilloscope. The oscilloscope has a bandwidth of 8 GHz and is capable of sampling at 40 GS/s. SkyCross omnidirectional antennas were used for transmitting and receiving the signals. The small dimensions of the antenna match the small dimensions requirements of on-body devices. The Agilent E8257D PSG analog signal generator provided the carrier signal at 2.4 GHz. Calibration was performed to compensate for the cable loss, connection mismatch, and other imperfections in the signal path from the antenna to the oscilloscope. To calibrate different input ports, all receivers were placed at a known distance (0.5 m) and the signals were compensated to be the same as channel 1 in the peak amplitude.

The antennas were fixed against body using a dielectric band with a dielectric constant close to the air dielectric constant to prevent unwanted reflections. A dielectric material matching the air dielectric constant with thickness of 2 mm was used to distant the antenna from the skin surface. All measurements were performed in a room with the area of $2.76 \text{ m} \times 4.5 \text{ m}$. Fig. 4 depicts the map of the room, furniture, and equipments arrangements.

A. Distribution of the Channel Gain

Assume that a wireless device (S) is attached to the left wrist which has high mobility. It can be a pulse sensor, a blood pressure sensor, or a motion sensor with clinical or recreational applications. The device is sending packets to the hub (H) on the right side of the waist which is usually larger and has more power and computational resources to be logged or retransmitted to a data center or clinic. H can be a mobile phone, PDA, or a dedicated device. This configuration is a typical example of the futuristic applications of an on-body network where wireless modules could be embedded in devices used in everyday life such as wrist watch and mobile phones. Measurements show that the best candidate locations for relaying the wrist node packets are nodes R_1 and R_2 as shown in Fig. 5. This is because, both R_1 and R_2 have constant connection with both S and H .

The experiments were performed while the subject mimicked walking for about 17 s where 250 samples of the channel responses were captured during this time. Fig. 6(a) shows the channel gain variation for R_2 - H path.

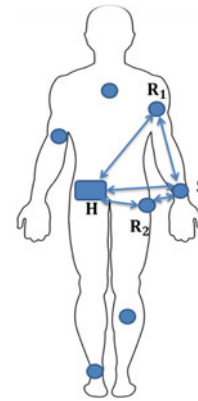


Fig. 5. Measured on-body links.

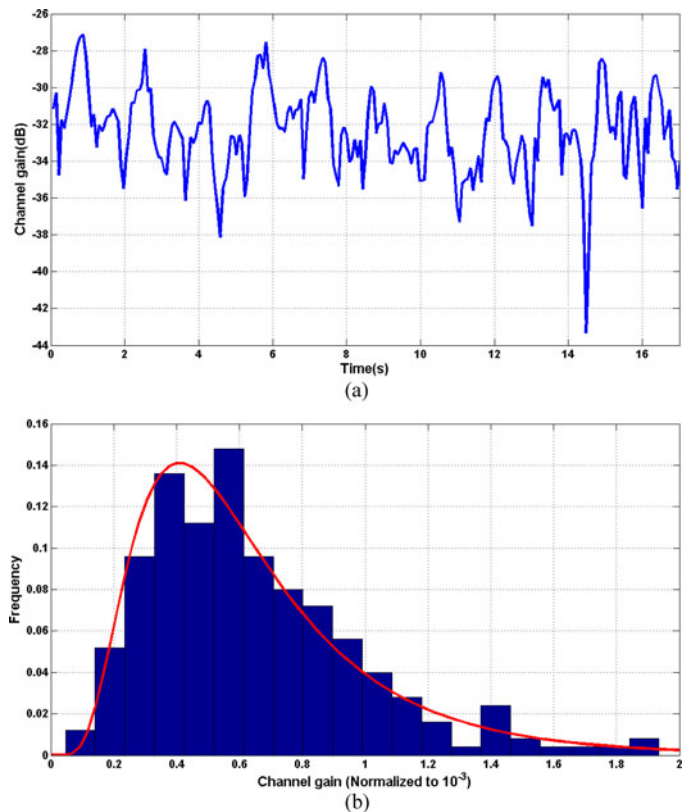


Fig. 6. Channel gain variations and its distribution. (a) Channel gain variations. (b) Distribution of the channel gain variations.

The channel gains are obtained as the ratio of the received power to the transmitted power of the signal generator. Akaike information criterion (AIC) was used to score the candidate distributions for the variations of the channel gain. Log-normal, Rayleigh, and Rician were ranked using AIC. Based on AIC score, log-normal distribution is the best model for the statistics of the channel gain variations among other candidates which is in accordance with the measurement results reported in [22]. Fig. 6(b) shows log-normal distribution fitting to the channel gain variations of R_2 - H link. Parameters of the log-normal distribution for the measured links are given in Table I.

TABLE I
PARAMETERS OF THE LOG-NORMAL DISTRIBUTION OF CHANNEL GAIN
VARIATION AT 2.4 GHz

Channel	μ	σ
$S-H$	-8.364	1.043
$S-R_1$	-7.396	0.463
$S-R_2$	-7.515	0.716
R_1-H	-8.124	0.472
R_2-H	-7.489	0.558

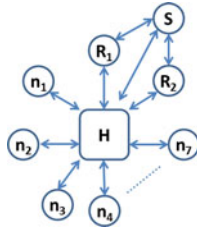


Fig. 7. Topology of the network.

Channel coherence time is a measure of how fast the channel is changing. Channel coherence time is calculated through the following equation [23]:

$$T_c = \sqrt{\frac{9}{16\pi}} \frac{1}{f_d}, \quad (42)$$

where f_d is the maximum Doppler frequency and is defined as

$$f_d = f_0 \frac{v}{c} \cos(\theta), \quad (43)$$

where $v \cos(\theta)$ is the component of the relative velocity of the transmitter in the direction of the receiver. This is important because, depending on the rate of the channel variations, different frames in a session may experience different channel qualities. The fastest moving node in our experimental setting is the wrist node during walking measurements with a maximum velocity of about 0.7 m/s toward the hub. The estimated channel coherence time for the link between S and H is about 76 ms while the longest session is a successful transmission to a relay in the adaptive scheme. The time it takes for this session to complete is about 2.1 ms which is much shorter than the estimated channel coherence time. Hence, it is safe to assume that the channel quality remains constant during one communication session.

IV. RESULTS AND COMPARISON

In this section, the mathematical energy model derived in Section II is evaluated through simulation and compared for adaptive, single-hop and two-hop scheme. The network topology is shown in Fig. 7. In the figure, S is the source node and R_1 and R_2 are the two relays associated with S . The network has ten nodes (N_n) in total.

The suggested modulation in the standard [8] for 2.4-GHz carrier is $\pi/4$ -DQPSK at 600 ksymbol/s. Parameters of the system are given in Table II.

TABLE II
SYSTEM PARAMETERS

Parameter	Value [8], [24]
Carrier Freq.	2.4GHz
Modulation	$\frac{\pi}{4}$ -DQPSK
Symbol Rate	600ksym/sec
$SIFS$	75 μ sec
$CIFS$	100 μ sec
TO	30 μ sec
β	145 μ sec
N_n	10
N_r	2
w_0	8
w_m	32
m	5
r_m	5
e_b	10^{-6}
P_{rx}	52 μ W
α_0	1.28×10^{-4}
L	1024 bits

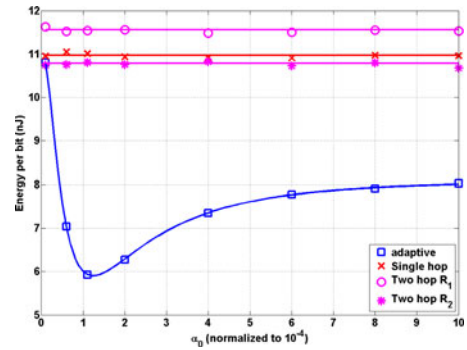
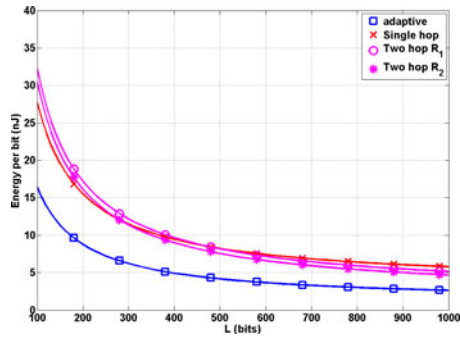
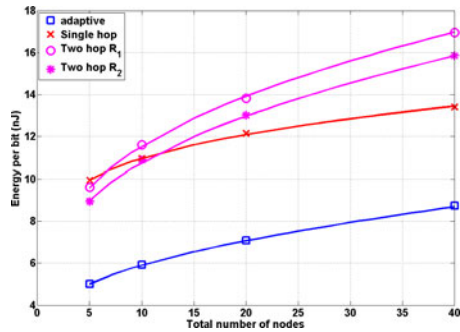


Fig. 8. Energy cost per bit versus α_0 .

In the evaluation of the mathematical model and simulations discussed below, values of the parameters are set as given in the Table II unless the parameter is a variable. Simulations are implemented in MATLAB using the rules described in Section II, parameters of the channel given in Table I, and parameters of the system given in Table II. In the following figures, solid line depicts the mathematical model prediction while markers indicate simulation points. As seen in the figure, the mathematical model can predict the simulation results with high accuracy.

Fig. 8 shows the total energy consumption per bit for different values of α_0 . Clearly, only the energy consumption of the adaptive protocol is a function of α_0 . As the figure shows, there is an optimum value for $\alpha_0 = 1.28 \times 10^{-4}$ where the energy consumption per bit is minimum $\bar{E}_{\text{adaptive}} = 5.90$ nJ/bit which is about 54.57% of the next minimum route $\bar{E}_{\text{Two-hop } R_2} = 10.81$ nJ/bit. At this threshold, the source node optimally switches between direct and relayed transmission strategies. In addition, the best relay path is chosen to minimize the transmission energy. The figure also confirms that the best strategy of routing data is depending on the channel conditions. As the figure shows, average energy consumption per bit for the two-hop scheme using relay 2 is lower than single hop as the channel quality of this relay is higher on the average. On the other hand, the energy consumption for the two-hop scheme using relay 1 is highest due to the less favorable channel conditions from R_1 to H as given in Table I and increased overhead


 Fig. 9. Energy cost per bit versus payload size (L).

 Fig. 10. Energy cost per bit versus number of nodes in the network (N_n).

of relayed routing. This would further confirm the advantage of the adaptive routing strategy to preserve the energy of the nodes. As α_0 approaches zero, the energy consumption of the adaptive scheme reaches single-hop energy as the relay is almost never used. On the other hand, for large values of α_0 , relay paths are used more frequently. The average energy cost for adaptive at higher values of α_0 is lower than the two-hop scheme for both relays because, adaptive routing chooses the best path to route its data and hence consumes less energy on the average.

Fig. 9 shows the energy consumption per bit versus increasing payload size (L). At small payload sizes, single hop transmission is better due to the less protocol overhead. The energy consumption per bit decreases by increasing the payload size which is mainly due to the reduced cost of protocol overhead relative to the payload. Another advantage of larger payload size is that for the same number of retries due to the collision of RTS packets, larger number of bits are transferred. Adverse effect of larger payload size is the increased packet error probability.

Fig. 10 shows that the energy cost of transmitting an information bit rises by increasing the number of nodes in the network. The main contributors to this rise in the energy cost are the higher number of collisions and longer waiting time before a successful contended session is obtained. The energy cost for two hop increases at a higher rate due to the contribution of energy consumption of the relay to the total energy cost. Unlike a generic sensor network, the number of nodes in a BAN is normally limited to a few nodes, e.g., less than ten nodes. However, investigating the effect of larger node numbers is interesting as in the future, such networks will share the medium with users of other BANs and the total number of the nodes can be large.

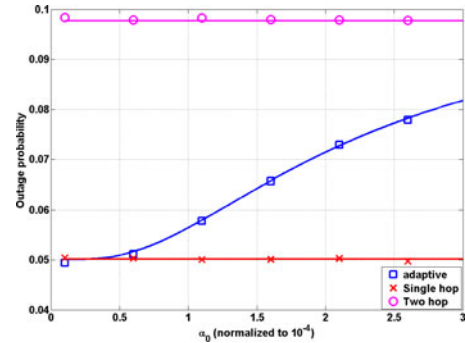
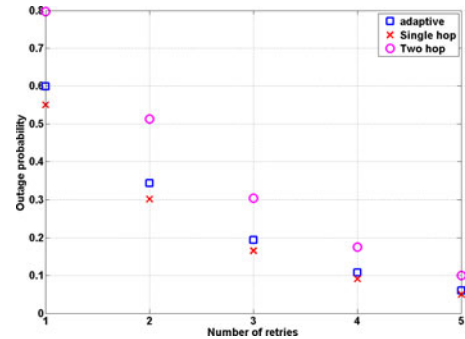

 Fig. 11. Outage probability versus α_0 .

 Fig. 12. Outage probability versus maximum retry limit (r_m).

Fig. 11 shows the probability of outage for the adaptive scheme as a function of α_0 . As seen in the figure, the two-hop scheme has the highest probability of the outage as it requires that both packet transfers from the source to relay and relay to hub to be successful. As expected, lower values of α_0 in adaptive routing result in outage probabilities similar to the single-hop scheme and as α_0 gets larger the outage reaches the two-hop scheme outage probability since the relays are used more often. Nevertheless, at the optimum channel quality threshold where the energy cost is minimized ($\alpha_0 = 1.28 \times 10^{-4}$), the outage probability of the adaptive scheme ($p_o^{\text{adaptive}} = 0.06$) is only slightly higher than the single-hop outage probability ($p_o^{\text{singlehop}} = 0.05$).

Increasing the maximum number of retries will decrease the dropped packets number and thus the outage probability as depicted in Fig. 12. This, however, results in higher energy consumption as shown in Fig. 13. Hence, there is a tradeoff between higher energy cost and lower outage probabilities.

Latency and error in channel gain estimation may lead to nonoptimal energy consumption. Latency in channel estimation is tolerated by the system within the channel coherence time as discussed in Section III. In practice, the channel gain is estimated using the preamble of the physical layer frame. The channel gain is usually estimated within the preamble time ($75 \mu\text{s}$) which is negligible comparing to the on-body channel coherence time (75ms). To investigate the effect of the error in channel estimation on the energy consumption in the adaptive protocol, an error was introduced to the estimated channel and the energy consumption was obtained. Fig. 14 shows the percentage of the increase in the energy consumption versus the percentage

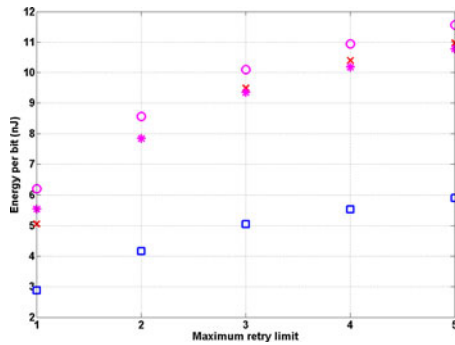


Fig. 13. Energy cost per bit versus maximum retry limit (r_m).

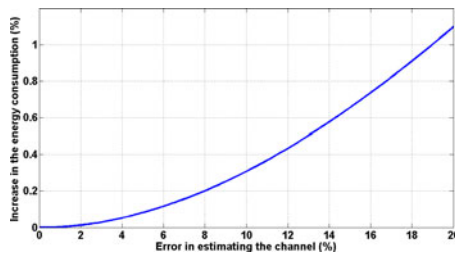


Fig. 14. Increase in energy consumption (%) versus error in channel estimation (%).

of the introduced error. The percentage for the energy and error in channel estimation was obtained relative to the energy consumption and channel gain in a perfect channel estimation condition at the source node. As seen in the figure, up to 2% error in channel estimation has no significant effect on the energy consumption and 20% error in channel estimation would increase the average energy consumption per bit by approx. 1%.

V. CONCLUSION

In this paper, we addressed the energy cost of transmitting a bit of information in dynamic human body setting. An adaptive scheme is proposed to improve the energy efficiency of the nodes in the network. The key idea is to adaptively change the routing strategy based on the quality of the channel. The adaptive protocol is mathematically analyzed based on the medium access procedures of the IEEE 802.15.6 standard and the analytical model is validated through simulations. The adaptive scheme is then compared with the existing method and it is shown that the adaptive routing can reduce the energy cost of information bit by 54%.

REFERENCES

- [1] M. Chen, S. Gonzalez, A. Vasilakos, H. Cao, and V. Leung, "Body area networks: A survey," *Mobile Netw. Appl.*, vol. 16, no. 2, pp. 171–193, 2011.
- [2] A. Pantelopoulou and N. Bourbakis, "A survey on wearable sensor-based systems for health monitoring and prognosis," *IEEE Trans. Syst., Man, Cybern. C, Appl. Rev.*, vol. 40, no. 1, pp. 1–12, Jan. 2010.
- [3] B. Latré, B. Braem, I. Moerman, C. Blondia, and P. Demeester, "A survey on wireless body area networks," *Wireless Netw.*, vol. 17, no. 1, pp. 1–18, 2011.
- [4] S. Ullah, X. An, and K. S. Kwak, "Towards power efficient MAC protocol for in-body and on-body sensor networks," in *Agent and Multi-Agent Systems: Technologies and Applications*. New York, NY, USA: Springer-Verlag, 2009, pp. 335–345.
- [5] X. Liang and I. Balasingham, "Performance analysis of the IEEE 802.15.4 based ECG monitoring network," in *Proc. 7th IASTED Int. Conf. Wireless Opt. Commun.*, 2007, pp. 99–104.
- [6] N. Timmons and W. Scanlon, "An adaptive energy efficient MAC protocol for the medical body area network," in *Proc. 1st Int. Conf. Wireless Commun., Veh. Technol., Inf. Theory Aerosp. Electron. Syst. Technol.*, 2009, pp. 587–593.
- [7] B. Braem, B. Latre, I. Moerman, C. Blondia, E. Reusens, W. Joseph, L. Martens, and P. Demeester, "The need for cooperation and relaying in short-range high path loss sensor networks," in *Proc. Int. Conf. Sens. Technol. Appl.*, 2007, pp. 566–571.
- [8] (2012). IEEE Standard for Local and metropolitan area networks—Part 15.6: Wireless body area networks. [Online]. Available: <http://standards.ieee.org/getieee802/download/802.15.6-2012.pdf>
- [9] C. Tachtatzis, F. Di Franco, D. C. Tracey, N. F. Timmons, and J. Morrison, "An energy analysis of IEEE 802.15.6 scheduled access modes for medical applications," in *Ad Hoc Networks*. New York, NY, USA: Springer-Verlag, 2012, pp. 209–222.
- [10] S. Ullah, M. Chen, and K. S. Kwak, "Throughput and delay analysis of IEEE 802.15.6-based CSMA/CA protocol," *J. Med. Syst.*, vol. 36, no. 6, pp. 3875–3891, 2012.
- [11] S. Rashwand, J. Mistic, and H. Khazaei, "IEEE 802.15.6 under saturation: Some problems to be expected," *J. Commun. Netw.*, vol. 13, no. 2, pp. 142–148, 2011.
- [12] S. Ullah and K. S. Kwak, "Throughput and delay limits of IEEE 802.15.6," in *Proc. IEEE Wireless Commun. Netw. Conf.*, 2011, pp. 174–178.
- [13] F. Martelli, C. Buratti, and R. Verdone, "On the performance of an IEEE 802.15.6 wireless body area network," in *Proc. 11th Eur. Wireless Conf.—Sustainable Wireless Technol.*, 2011, pp. 1–6.
- [14] N. Bradai, S. Belhaj, L. Chaari, and L. Kamoun, "Study of medium access mechanisms under IEEE 802.15.6 standard," in *Proc. 4th Joint IFIP Wireless Mobile Network Conf.*, 2011, pp. 1–6.
- [15] N. F. Timmons and W. G. Scanlon, "Improving the ultra-low-power performance of IEEE 802.15.6 by adaptive synchronisation," *IET Wireless Sens. Syst.*, vol. 1, no. 3, pp. 161–170, 2011.
- [16] B. H. Jung, R. U. Akbar, and D. K. Sung, "Throughput, energy consumption, and energy efficiency of IEEE 802.15.6 body area network (BAN) MAC protocol," in *Proc. IEEE 23rd Int. Symp. Pers. Indoor Mobile Radio Commun.*, 2012, pp. 584–589.
- [17] S. Rashwand, J. Mistic, and H. Khazaei, "Performance analysis of IEEE 802.15.6 under saturation condition and error-prone channel," in *Proc. IEEE Wireless Commun. Netw. Conf.*, 2011, pp. 1167–1172.
- [18] A. Maskooki, C. B. Soh, E. Gunawan, and K. S. Low, "Ultra-wideband real-time dynamic channel characterization and system-level modeling for radio links in body area networks," *IEEE Trans. Microw. Theory Techn.*, vol. 61, no. 8, pp. 2995–3004, Aug. 2013.
- [19] (2012). IEEE Standard for Information technology, Telecommunications and information exchange between systems local and metropolitan area networks. [Online]. Available: <http://standards.ieee.org/getieee802/download/802.11-2012.pdf>
- [20] G. Bianchi, "Performance analysis of the IEEE 802.11 distributed coordination function," *IEEE J. Sel. Areas Commun.*, vol. 18, no. 3, pp. 535–547, Mar. 2000.
- [21] M. Ergen and P. Varaiya, "Throughput analysis and admission control for IEEE 802.11 a," *Mobile Netw. Appl.*, vol. 10, no. 5, pp. 705–716, 2005.
- [22] K. Yazdandoost and K. S. Pour. (2009). Channel model for body area network (BAN): IEEE P802.15-08-0780-09-0006. [Online]. Available: <https://mentor.ieee.org/802.15/dcn/08/15-08-0780-04-0006-tg6-channel-model.pdf>
- [23] T. S. Rappaport, *Wireless Communications: Principles and Practice*, 2nd ed. ed. Englewood Cliffs, NJ, USA: Prentice-Hall, Jan. 2002.
- [24] N. Pletcher, S. Gambini, and J. Rabaey, "A 52 μ W wake-up receiver with 72 dBm sensitivity using an uncertain-IF architecture," *IEEE J. Solid-State Circuits*, vol. 44, no. 1, pp. 269–280, Jan. 2009.

Authors' photographs and biographies not available at the time of publication.